

THE BINDING OF THE RADIOPROTECTIVE AGENT CYSTEAMINE WITH THE PHOSPHOLIPIDIC MEMBRANE HEADGROUP-INTERFACE REGION

FRANÇOIS BERLEUR,* VINCENT ROMAN,† DONALD JASKIEROWICZ,† MARC FATOME,†
FRANÇOIS LETERRIER,‡‡ LISBETH TER-MINASSIAN-SARAGA§ and GEORGETTE
MADELMONT§

*Centre d'Etude Nucléaire, Département de Physicochimie, Section de Chimie Moléculaire, 91191
Saclay Cedex, France; †Division de Biophysique, Division de Radiobiologie et Radioprotection du
Centre de Recherche du Service de Santé des Armées, F 92141 Clamart, France; §Physicochimie des
Membranes et des Surfaces, UER Biomédicale, 45 rue des Saints Pères, F 75270 Paris Cedex 06, France

(Received 22 November 1984; accepted 8 March 1985)

Abstract—The interaction of the aminothioliol radioprotector cysteamine (β -mercaptoethylamine) (CYST) with dipalmitoylphosphatidylcholine (DPPC) artificial membranes has been studied by differential scanning calorimetry (DSC), turbidimetry and spin labeling. This hydrophilic molecule displays a biphasic, concentration-dependent binding to the phospholipidic head groups at neutral pH.

In the CYST/DPPC molar ratio 1:160–1:2 (mole/mole) an increasing ordering effect is observed. At high concentrations (over 3:1 ratio), this ordering effect decreases. With the symmetric disulfide dimer cystamine, the biphasic effect is not shown and the membrane rigidity decrease is obtained only at concentration ratio higher than 1:1.

The charge repartition of the cysteamine molecule has been shown to be disymmetric, +0.52 e on the NH_3 group and +0.19 e on the SH extremity, [38] whereas the cystamine molecule is electrostatically symmetrical. These properties could be related to their membrane effects. With cysteamine, at a low concentration, an electrostatic bridging between the negatively charged phosphate groups of the polar heads induces the increase in membrane stability: the molecules behave like a divalent cation. At high concentrations a displacement of the slightly charged SH extremity by the amine disrupts the bridges and induces the decrease in rigidity: the drug behaves like a monovalent cation. Due to its symmetric charge and its double length, such an effect is not observed with cystamine.

This study could bring further information about the interactions between cysteamine and polyelectrolytic structures (ADN for example) and about the radioprotective properties of this drug.

The hydrophilic molecule cysteamine (β -mercaptoethylamine) is known as an aminothioliol radioprotective agent since its discovery in the 1950s. It has been used in many radiobiology studies *in vivo* [1] and can be considered as a standard among sulfur-containing molecules. A variety of hypotheses have been advanced to explain its properties [1, 2]. Among the most important of them may be listed an inhibition of free radical process [3] by acting as a radical scavenger, a protection by hypoxia or anoxia by decreasing O_2 consumption in the cell [4] and control of DNA breakdown, by electrostatic attachment to the polyelectrolytic DNA molecule [5].

It has also been suggested that the biological membranes could represent a critical target for ionizing radiation and several authors have proposed an interaction between cysteamine and biological phospholipid structures [6].

Furthermore, in previous experiments, we have demonstrated that the radioprotective effect of cysteamine is strongly modified when encapsulated in liposomes [7]. Although the dose reducing factor (DRF) is not significantly changed, the duration of the biological action is considerably increased (up to 3 hr instead of 20 min) and the encapsulated drug

becomes active when orally given, which is not the case for the free compound in solution.

Several authors have already pointed out that many drugs belonging to various pharmacological groups, i.e. phenothiazines [8, 9], tricyclic antidepressants [10], local anesthetics and others [11], affect the physico-chemical properties of lipid bilayers [12, 13]. In particular, the molecules containing a hydrophobic portion and a short side chain with a protonized amino group bind to phospholipidic membranes [14, 15]. These drugs intercalate between the lipid molecules, the cationic group being located near the polar head group of the phospholipids while the hydrophobic part points toward the hydrophobic core of the bilayer.

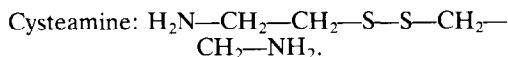
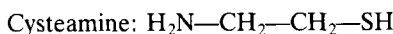
In an attempt to explore the interaction of cysteamine and its dimeric form cystamine with the membrane bilayer, a study with an artificial model membrane has been undertaken. The effects of these cationic amphiphilic drugs are described by the thermal behaviour of the drug-DPPC mixtures and by dose/effect relationship plots. Three complementary methods, differential scanning calorimetry (DSC), turbidimetry and electron spin resonance (ESR) have been used in this work.

Turbidimetry and DSC reveal the thermodynamic state of the membrane taken as a whole [2, 16–18]

‡ To whom all correspondence should be addressed.

whereas spin labeling provides a description of the local ordering and/or fluidity of the phospholipid acyl chains, with a spatial resolution of about 0.5 nm [19, 20].

In this work, we present results carried out on fully hydrated (90% w/w water) DPPC multibilayers (liposomes), in the absence (control) and in the presence of variable concentrations of cysteamine or its S-S dimer, cystamine.



MATERIALS AND METHODS

Reagent and sample preparation. Synthetic L- α -dipalmitoyl phosphatidylcholine (DPPC) of 99% purity was purchased from Sigma. The purity was checked by thin layer chromatography.

Cysteamine hydrochloride and cystamine hydrochloride were purchased from Merck, Sharp and Dohme, West Point PA.

The DPPC samples were prepared according to Bangham [21] in a 10 mM phosphate buffer at pH 7.0. Cysteamine or cystamine were added at different concentrations, from 10^{-4} to 10^{-1} M. The DPPC-drug mixture was then incubated at 50° for 30 min.

For spin label experiments, the multibilayer liposomes were labeled with *N*-oxyl-oxazolidine derivatives of stearic acid, named, respectively, 5-NS, when the nitroxide group is located on the 5th carbon, and 16-NS, when located on the 16th carbon, the carbon being counted from the carboxylic acid group.

DSC experiments. The DSC scanner was a Du Pont de Nemours thermoanalyser 990.910 equipped with a mechanical cooling accessory. Scanning was performed between 5 and 60° at the heating rate of 2 K/min. The peak characteristics are designated by their onset and maximum temperature. The heats involved were related to the peak area by using a planimeter.

Spectrophotometry. The investigation described here was performed using a Beckman DU-8 spectrophotometer equipped with the Tm Analysis System. By this arrangement it was possible to make sequential measurements of absorbance at 450 nm vs temperature. In this experiment, the absorbance *A* was measured as a function of the temperature. For a non-absorbing but light-scattering system, we can define the turbidity *T* for a 1-cm path-length by:

$$T = -\ln I/I_0 = -2.303 \log I/I_0 = 2.303 A \quad [22].$$

It is a measure of the integrated intensity of light scattered at all angles. *I*₀ is the incident intensity, *I* the intensity of the transmitted light and *A* the measured absorbance.

Spin-label experiments. To 200 μ l of the suspension, 5 μ l of a 10 mM stock solution of spin label in dimethyl sulfoxide was added. The label/DPPC molar ratio was about 1/1000. The sample was incubated for 30 min at 50° (above the melting point) in order to allow the penetration of the probes.

Electron spin resonance spectra were recorded in the temperature range 0–60° at about 1° intervals

using a Varian E109 spectrometer equipped with a laboratory-built temperature controller (accuracy $\pm 0.2^\circ$).

The principles of interpretation of spin label spectra have been developed in numerous studies [23, 24]. We shall only recall the definitions of the parameters we have measured.

The outer hyperfine splitting $2A_{\parallel}$ is used as a relative measurement of the rigidity on the system. For randomly oriented samples, the magnitude of $2A_{\parallel}$ generally decreases according to the motional freedom along the hydrocarbon chains.

When the inner hyperfine splitting $2A_{\perp}$ can be measured, which is the case when the fluidity of the lipidic bilayers becomes sufficiently high, the polarity of the spin label environment can be determined by the value of the splitting constant $a_N = 1/3 (A_{\parallel} + 2A_{\perp})$; the lower the polarity, the lower the value of this parameter.

However, in this work we were led to use particular parameters obtained from the saturation transfer technics (ST-ESR). In fact, the wobble motion of the spin label acyl chain around their molecular long axis is characterized by the correlation time τ_c and can be evaluated with a reasonable accuracy by the formula of Keith [25]. Such a formula is only available for τ_c values under 10^{-8} sec. To extend the motional sensitivity of the ESR technics to slower correlation times, we have performed saturation transfer [26]. Hyde and Dalton [27] have shown that the L''/L ratio is inversely correlated to τ_c (10^{-8} , 10^{-6} sec) where *L* and *L''* are, respectively, the amplitudes of the first and second peak of the ST-ESR spectrum, measured from the baseline (Fig. 9).

A DPPC/spin label control has been performed in order to check that fatty acid nitroxides do not modify the thermal behaviour of the liposomes.

RESULTS

DSC experiments

Figure 1 represents the thermograms obtained in

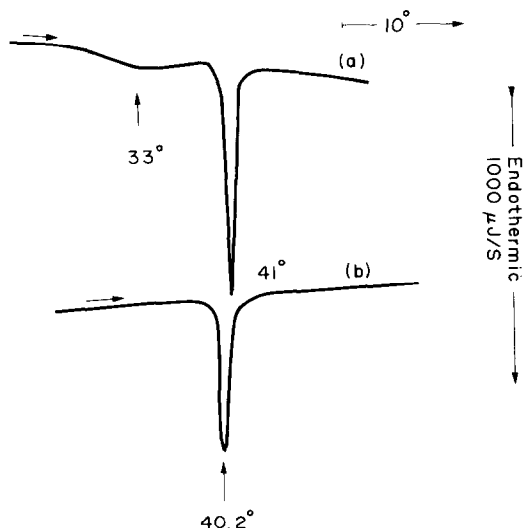


Fig. 1. DSC thermograms of fully hydrated (90%, w/w) DPPC bilayers. (a) Control DPPC. (b) Mixed cysteamine/DPPC, molar ratio $\rho = 0.5$.

Table 1. Experimental values of the DSC parameter obtained from the thermograms

	T_P	T_S	T_L	T^{\ddagger}	ΔH_c	ΔH_t	n_c	n_t
Control DPPC	33	40.5	41	1.1	7.7	9.6	187	150
Cysteamine	a	39.6	40.2	1.5	12.5	12.5	85	85

T_P , Pretransition temperature; T_S , solidus temperature; T_L , liquidus temperature; T^{\ddagger} , transition half-width; ΔH_c , main transition molar enthalpy; ΔH_t , total transition molar enthalpy; n_c , co-operativity number obtained from ΔH_c ; n_t , co-operativity number obtained from ΔH_t ; a, no transition observed.

heating the fully hydrated pure DPPC (control, a) and the mixed cysteamine/DPPC (molar ratio $\rho = 0.5$). The comparative experimental parameters are presented in Table 1. We observe that in the presence of cysteamine, the pretransition peak disappears and the main transition is down-shifted from 41° (control) to 40.2°, and 35% broadened. Furthermore, the molar enthalpy of the total transition is about 1.3-fold enhanced.

According to Mabrey and Sturtevant [28], the co-operativity number for the main transition can be evaluated by:

$$n_t = 6.9 T_m^2 / T^{\ddagger} \times 1 / \Delta H_t,$$

where T^{\ddagger} is the transition half-width, T_m the midpoint of T^{\ddagger} and ΔH_t the transition molar enthalpy. For $\rho = 0.5$, n_t is 40% lowered compared to the control (Table 1).

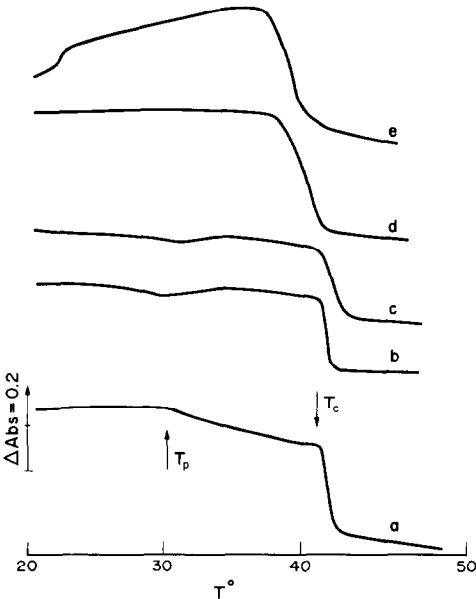


Fig. 2. Plot of the absorbance values vs temperature. (a) Control DPPC (10^{-3} M). (b) Cysteamine/DPPC, molar ratio: 0.075. (c) Cysteamine/DPPC, molar ratio: 0.75. (d) Cysteamine/DPPC, molar ratio: 7.5. (e) Cysteamine/DPPC, molar ratio: 75.

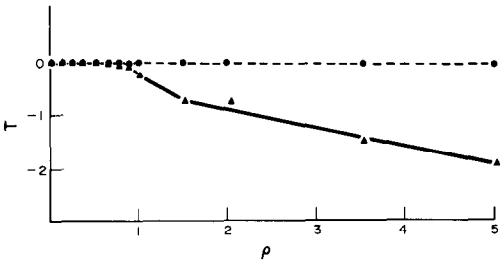


Fig. 3. Variation in ° of the main transition temperature vs the molar ratio for (▲) mixed cysteamine/DPPC and (●) mixed cysteamine/DPPC.

Spectrophotometry

This method follows the changes in turbidimetry (absorbance). The measurements were partly prompted by the findings that light scattering and turbidimetry are sensitive to phase transition in DPPC liposomes. The physical basis of absorbance changes at the main-phase transition comes from a partial change in the molar volume \bar{v} of the lipid, which leads to a change in the specific refractive index increment dn/dc (where c is the concentration) and hence in light scattering [29, 30]. If all turbidity changes observed with liposome samples are only due to density changes, the measurable effect at the pretransition temperature suggests that there is a small change in \bar{v} of the bilayer, presumably by uptake of water [30, 31].

Figure 2a is a plot of the absorbance values at 450 nm of a pure lipidic suspension (1 mg/ml) vs temperature. Both transitions are clearly displayed at 42° and around 32°. For a low cysteamine concentration (10^{-4} M, Fig. 2b), the pretransition is not precisely defined and the main transition remains similar to the control. At 10^{-3} M (Fig. 2c), the pretransition vanishes while the main transition broadens. At higher concentration (DPPC/drug molar ratio 10^{-2} and 10^{-1} M, respectively, Figs 2d and e), a more dramatic broadening and a down-shift of the main transition is observed. In Fig. 3, the main transition temperatures are plotted versus ρ in the

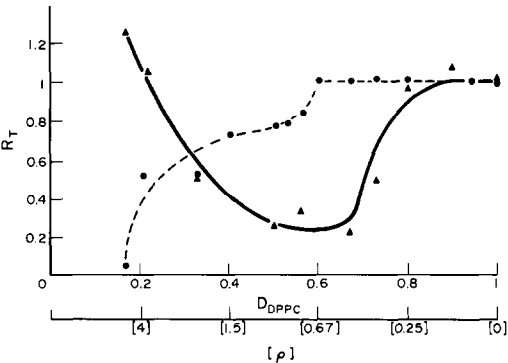


Fig. 4. R_T values as a function of cysteamine and cystamine concentration. × DPPC, Molar fraction; ρ , molar ratio; ▲, cysteamine; ●, cystamine.

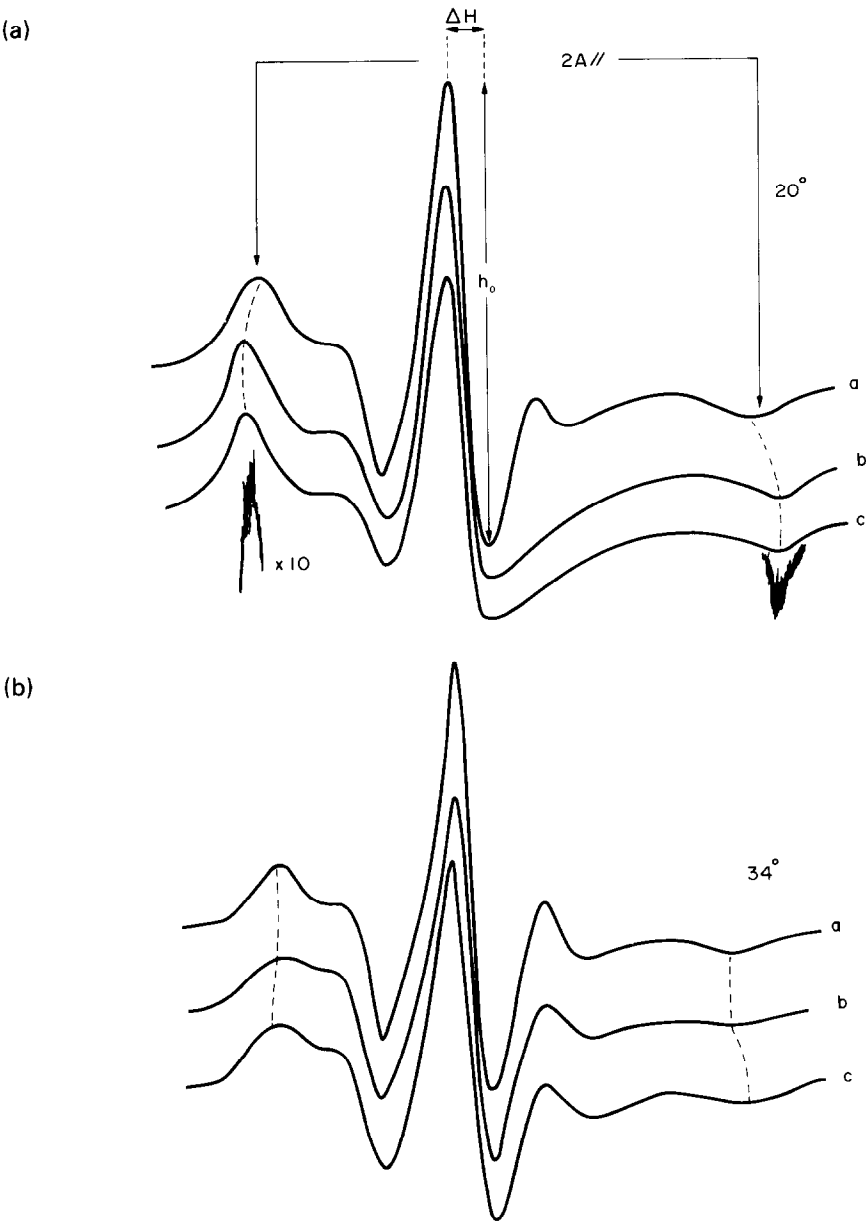
Table 2. Characteristic values of the spectral parameters measured with 5-NS as a function of pH. $A_{||}$ is the hyperfine component, a_N is the isotropic coupling value

$T = 50^\circ$	pH 2.9 (COOH)	pH 9.9 (COO ⁻)	pH 7.0 cysteamine
$2A_{ }(\text{mT})$	4.125	4.925	4.140
a_N	1.410	1.470	1.415

presence of cysteamine or cystamine. No change can be observed with cystamine.

The variations of absorbance at 450 nm which accompany the transition, reflect the changes of

shape and structure of the liposomes and provide information on the “stability” of the phospholipidic structures. In fact we can assume a strong correlation between the transition step amplitude and the change



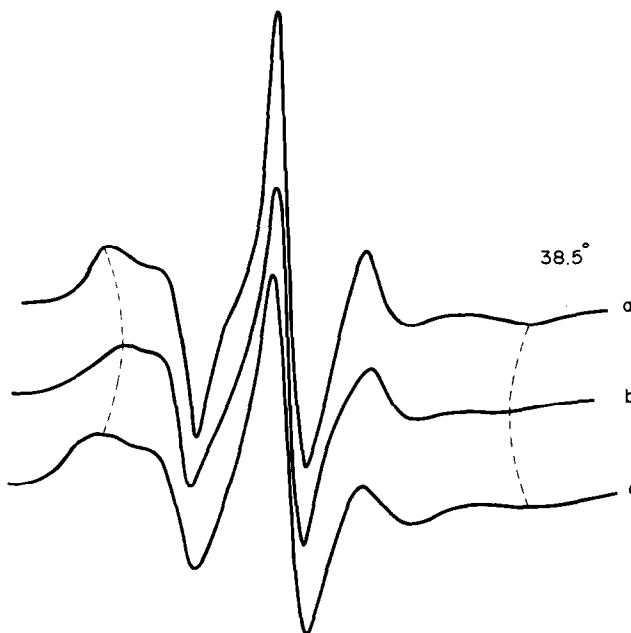


Fig. 5. Spectra obtained with 5-NS spin label at 20, 34 and 38°. (a) Control DPPC, pH 7.0. (b) Mixed cysteamine/DPPC, $\rho = 0.5$. (c) Mixed cysteamine/DPPC, $\rho = 1.5$.

in the density of the lipid. In order to describe the absorbance curves quantitatively we define the following ratio:

$R_T = T(20^\circ) - T(50^\circ)$ for a given cysteamine concentration / $T(20^\circ) - T(50^\circ)$ for pure DPPC.

The results are listed in Fig. 4.

A decrease in the transition step of R_T values is manifest between $\rho = 0.37$ and 2 and could be related to a "stabilizing" effect of cysteamine on the lipidic bilayer. The outstanding fact that a minimum value is observed for $\rho = 0.5$ will be discussed further.

In the presence of cysteamine, changes in the R_T

values are not revealed within the concentration range of $\rho = 0-75$. Furthermore, for a value of ρ above 0.75, R_T values decrease. We must point out the differences observed between the effects induced by cysteamine and its S—S-bridged dimer. At a low concentration the effects of cysteamine are much stronger than those induced by cysteamine and for that drug, no minimum is observed on the plot of R_T vs ρ .

Electron spin resonance experiments

5-NS spin label. This spin label probes the phospholipidic bilayer just above its polar groups.

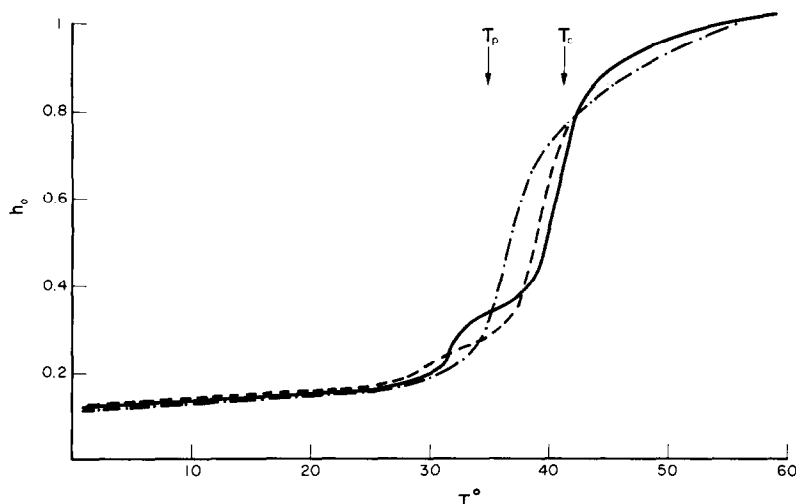


Fig. 6. Plot of the central line amplitude h_0 , measured on the 5-NS spectra, as a function of the temperature. The parameter h_0 is given in normalized arbitrary units (see Fig. 5). —, Control DPPC; ---, mixed cysteamine/DPPC, $\rho = 0.5$; — · —, mixed cysteamine/DPPC, $\rho = 37.5$. The main transitions observed on the DSC thermograms are indicated by arrows.

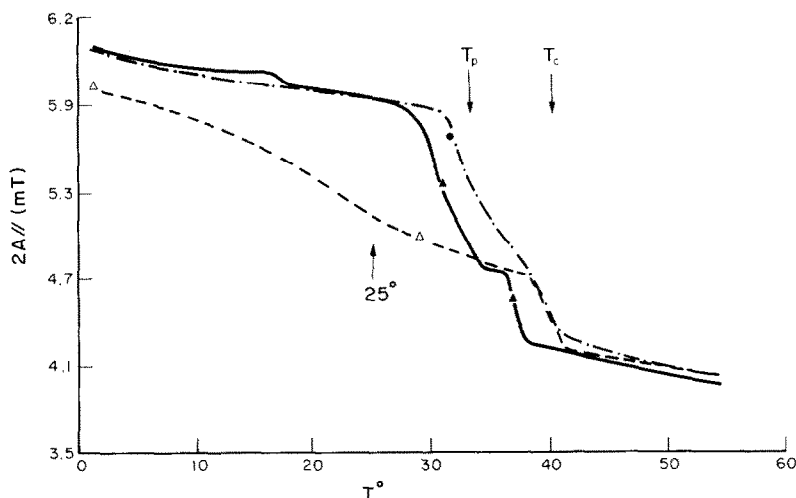


Fig. 7. Plot of the $2A_{||}$ parameter measured on the 5-NS as a function of the temperature. — Δ —, Control DPPC; — \blacktriangle —, mixed cysteamine/DPPC, $\rho = 0.5$; — \bullet —, mixed cysteamine/DPPC, $\rho = 1.5$.

The anchoring sites of the label carboxylic groups are pH-dependent as shown by the different values of $2A_{||}$ and a_N displayed at 50° and at pH 2.9 and 9.9, respectively (Table 2). Figure 5 shows characteristic spectra obtained at various temperatures and pH 7.0 which indicate a strongly immobilized system in the range 2–32° and a much more fluid system around 38°.

The plot (Fig. 6) of the spectrum central line vs T clearly displays the phase transition of the bilayer. In the presence of cysteamine ($\rho = 1.5$) no change in the transition temperature is observed; the same experiment performed with cysteamine ($\rho = 0.5$ and $\rho = 37.5$) reveals a clear decrease in the gel/liquid transition temperature. The down-shift of the main transition is about 2.0° with $\rho = 0.5$ and 4.5° with $\rho = 37.5$.

The variations of the $2A_{||}$ parameter T for the control at pH 7.0 (open triangles), the DPPC/cysteamine mixture ($\rho = 0.5$, full triangles) and the DPPC/cysteamine mixture ($\rho = 1.5$, full circle) are plotted in Fig. 7. In the temperature range 0–29° in the $L\beta'$ gel phase, the $2A_{||}$ values clearly stand above the control for the mixed drug/DPPC. A strong decrease is observed between 29° and 34° and the curve is superimposed on the control for about 2° for cysteamine. After a smooth decrease between 36 and 38°, the $2A_{||}$ values remains similar to the control.

Except a slight translation of 2.5° (main transition at 38.5° with cysteamine and 41° with cysteamine), both cysteamine and cysteamine- $2A_{||}$ temperature variations are similar, the second transition step on the cysteamine curve actually being the main transition.

At first sight, cysteamine interacts essentially with the phospholipid polar head groups. We have seen above (spectrophotometry) that cysteamine has a strong influence on the membrane structure in the $L\beta'$ gel phase. Such an effect is clearly revealed by spin labeling techniques.

In order to see whether this effect was concentration-dependent, we have plotted the relative

variation of the outer hyperfine splitting ($\Delta_r A_{||}$) vs cysteamine concentration at 25° (Figs 8a, b), temperature at which the maximal gap is observed in the $2A_{||}$ parameter between cysteamine or cysteamine and the control. A change in $\Delta_r A_{||}$ is revealed from $5.8 \cdot 10^{-3}$ M and an increase in the concentration induces

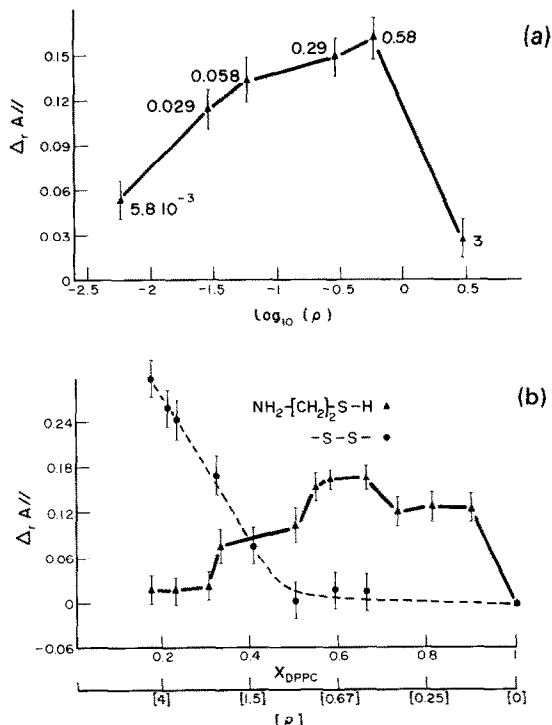


Fig. 8. Relative variation of the outer hyperfine splitting $2A_{||}$ vs cysteamine or cysteamine concentration. (a) Plot in logarithmic scale [$\log(\text{molar ratio})$]. The molar ratio is indicated for each value. (b) plot around $\rho = 0.5$ in decimal scale. \blacktriangle , Mixed cysteamine/DPPC; \bullet , mixed cysteamine/DPPC.

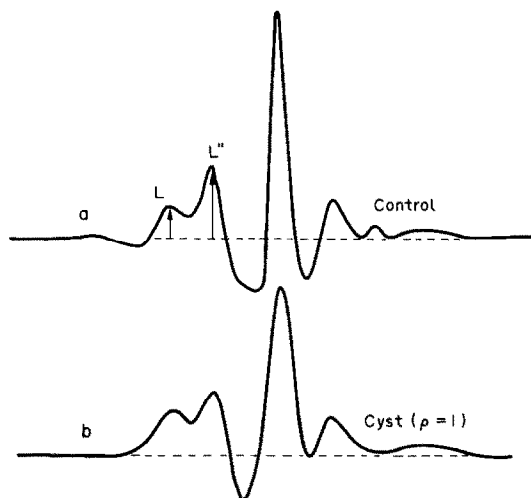


Fig. 9. ST-ESR spectra obtained with the 5-NS spin label. (a) Control DPPC. (b) Mixed cysteine/DPPC $\rho = 1$.

a correlated change until a maximum is reached for ρ_m around 0.5. An enlargement of this plot is presented on Fig. 8b, in the $\rho = 4-0$ concentration range. The maximum is still reached for ρ_m between 0.5 and 0.66. Between this value and $\rho = 2$ a sharp decrease of $\Delta_r A_{\parallel}$ is observed. Beyond this point the $2A_{\parallel}$ parameter remains constant. As compared to the control, this parameter does not overtake the baseline.

The same experiment has been performed with cysteine to check whether the membrane would behave alike in the presence of a symmetric and twice as large molecule. Values of $\Delta_r A_{\parallel}$, plotted vs ρ , (Fig. 8b) increase with the concentration from $\rho = 1$ but never reach a maximum value.

Additional information has been obtained from the evaluation of the tumbling rate τ_c of the spin label. Since τ_c was lower than 10^{-8} sec when observed by 5-NS labeling in a membrane gel phase, it was necessary to use ST-ESR techniques. The L and L'' parameters, as described by Hyde and Dalton [27], are presented on such a spectrum in Fig. 9. In the same way, the L''/L ratio has been plotted vs ρ in Fig. 10. The curve undergoes a sharp decrease until $\rho = 0.7$. Beyond this point, a slight increase is

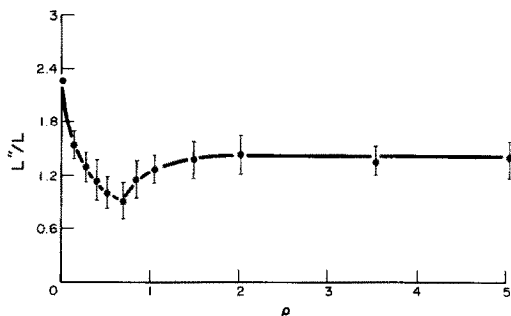


Fig. 10. Variation of the L''/L values (see Fig. 9) vs the molar ratio.

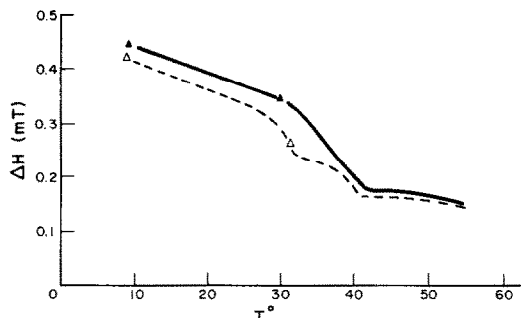


Fig. 11. Variation of the 16-NS central line half-width ΔH vs temperature. Δ , Control DPPC; \blacktriangle , mixed cysteine/DPPC, $\rho = 0.5$.

observed until $\rho = 2$ and the curve then remains approximately constant.

16-NS spin label. This spin label probes the DPPC bilayer near the methyl group of the acyl chain.

For mixed cysteine/DPPC ($\rho = 0.5$), the plot of h_0 (median field line amplitude) vs temperature (not presented) indicates that the main transition temperature and the transition half-width (co-operativity) are similar to the control. In addition, a pre-transition is revealed at 35° .

The effects in the transition-temperature range are further observed on the plot of ΔH vs T (Fig. 11). This parameter is correlated with the tumbling rate of the label (τ_c). Except for the end-point of the transition at 41° , the ΔH values remain above the control and both 35 and 40° transitions are clearly observed.

The $2A_{\parallel}$ parameter plotted vs T (not presented here) was proved to be similar to the control.

DISCUSSION

The fading of the pretransition observed by DSC and turbidimetry (Figs 1 and 2) reveals that cysteine and cystamine essentially interact with the DPPC membranes in their polar head region. The 60% enhancement in the main transition enthalpy ΔH_c indicates that the "fusion" of the acyl chains requires more energy and therefore that cysteine reinforces the structural organization of the membrane. This stabilizing effect is also revealed by turbidimetry in the decrease of the transition amplitude.

The increase in the transition width observed in turbidimetry and DSC and the decrease in the co-operativity number (DSC) could indicate the formation of domains induced by cysteine inside the DPPC structure.

The decrease in the main transition temperature only induced by cysteine could be correlated with the penetration of the relatively hydrophobic thiol group between the polar heads. An important effect involving the penetration of the thiol group inside the biological membranes has been previously described, which was proved to modify the local organization of the bilayer structure [32].

The preferential interaction of these drugs with the polar part of the DPPC bilayer, previously sug-

gested by Vasilescu [6], is further confirmed by the results obtained with spin labeling. In fact the 16-NS which probes the bilayer hydrophobic core shows practically no modification in the thermal behaviour of the membrane, whatever the drug concentration. Only a slight decrease in the acyl-chain tumbling rate is observed (increase in ΔH , Fig. 11), essentially in the intermediate transition range ($P\beta'$), which is a consequence of the structural modification of the polar heads region.

Both drugs induce a strong increase in the 5-NS $2A_{||}$ parameter, in the $L\beta'$ gel phase, below 30° . This reveals an increase in the rigidity of the phospholipidic structures near the polar heads. The second-order transitions observed at 29° with cysteamine and at 31° with cystamine can be interpreted as a modification of the $P\beta'$ structure induced by these drugs and could be correlated with the melting of DPPC-drug domains in the bulk of the bilayer. As we can see, the drugs do not in fact modify the structure in the $L\alpha$ phase above 41° , but this does not imply the absence of any interaction in the fluid state.

The anchoring of the spin-labeled fatty acids is pH-dependent according to the ionization state of the carboxylic group [33, 34]. The protonated form (COOH) penetrates more deeply inside the lipidic structure than the negatively charged COO^- . In the first case, the 5-NS $2A_{||}$ parameter is lower, and the isotropic hyperfine constant higher than for COO^- (Table 2). The apparent pK_a value of the carboxylic acids in the amphiphilic polar interface structure is 7.4. We can assume that the adsorption of the protonated cysteamine or cystamine near the DPPC polar heads induces a modification in the ionization state of the spin label in favour of the COO^- form. The results presented in Fig. 5 indicate that the modifications observed with the 5-NS spin label are not due to such a pH effect.

Cysteamine is a small-sized molecule. The distance between the sulfur atom and a hydrogen of the ammonium group is about 0.28 nm. By quantum mechanics, *ab initio* calculation of the net charge in proton unit has established that the cysteamine monocation possesses a NH_3 head with a strong positive charge (+0.52 e) and an SH tail with a weaker, but not negligible, charge (+0.19 e) [35]. At pH 7.0, both charged extremities may interact at the lipid/water interface with the negatively charged phosphate group.

The dissymmetry in the electric charges born by both cysteamine extremities could explain the biphasic shape in the plot of structure or fluidity-correlated parameters vs cysteamine concentration (Figs 8a, b). First the strongly charged NH_3 head group links onto a polar-interface phosphate group and, according to the steric distances, the SH tail is likely to interact with a contiguous phosphate site. This electrostatic bond can be responsible for the increase in the cohesive strength between phospholipidic molecules. Under this condition, it is of logical assumption to suggest a maximal organization ($2A_{||}$) and rigidity (τ_c) for $\rho = 0.5$, i.e. for the saturation of the phosphate-charged sites.

Such an enhancement in the packing reflects a parallel decrease in the molecular area, i.e. the mean

surface occupied by the phospholipidic molecule. The experimental results become clear if we assume that cysteamine interacts by weakening the electrostatic repulsion forces between the polar heads [36]. In fact at this concentration ($\rho = 0.5$) cysteamine behaves like a divalent cation.

Beyond this optimal concentration, the NH_3 group of a free cysteamine molecule must compete with an SH group of a bound molecule and induce a displacement of the weakly charged extremity. In this hypothesis, when all phosphate sites are bound to a cysteamine NH_3 head group ($\rho \geq 1$), the structural interface organization becomes independent from any further increase in the concentration. In fact the structure- and fluidity-related parameters cannot return to their previous values, according to the steric hindrance induced by cysteamine inside the polar interface. Such a phenomenon is actually observed on Fig. 8b. In this case cysteamine behaves like a monovalent cation.

In contrast cystamine is a symmetric molecule bearing equal charges at both extremities. By electrostatic binding, it can induce an increase in the rigidity of the bilayer structure in the same way (Fig. 8b). However, adsorption at the polar interface is more difficult on account of its larger dimensions (0.8 nm, i.e. 2-fold than cysteamine); thus for a $2A_{||}$ value assigned to cysteamine ($\rho = 0.5$ for example), cystamine requires a 3-fold higher concentration. By increasing the concentration, no competition appears between bound (weak) and free (strong) electrostatic charges and the variation of the $2A_{||}$ parameter still parallels the concentration (Fig. 8).

PHARMACOLOGICAL IMPLICATIONS OF THE PRESENT RESULTS

This report clearly demonstrates the strong interaction of cysteamine with DPPC bilayers, by the use of different experimental techniques. Moreover, according to the DPPC/cysteamine ratio, cysteamine behaves like a mono- or divalent cation, on account of the dissymmetry in the partitioning of its electrostatic charges. This hypothesis is reinforced by the completely different behaviour of cystamine, the charge of which being equally partitioned.

It is difficult to extrapolate the results obtained on DPPC bilayers to biological membranes. However, an electrostatic binding may contribute to give a partial explanation of the mechanism of the radio-protective effect. Some of the earliest biological damage induced by ionizing radiations are:

(1) the creation of free radicals produced from water molecules and reacting with membrane phospholipids and membrane-dependent enzymatic systems, and inducing (2) single- or double-strand breakdown in DNA molecules, all these damages being enhanced by the oxygen concentration.

In a well-known process cysteamine would act by scavenging free radicals released in biological structures, by transferring hydrogen atoms from thiol- to radiation-induced radicals created from water or formed on proteins and peptides. This effect has been clearly demonstrated in the repair of neuro-degenerative damages involving hydroxyl radicals and induced in peripheral adrenergic nerves by 6-OHDA [37].

But many thiols do not protect and most thiols are theoretically capable of forming mixed disulfides. Many biological investigations have demonstrated that more than a 3-carbon distance between the amine and the thiol functions leads to non-protective aminothiols. Vasilescu and Rix-Montel [5] have demonstrated the theoretical possibility of a reversible electrostatic binding of cysteamine molecules on the portion of the DNA helix unprotected by histones. We have shown experimentally that the cationic parts of such a radioprotective agent are electrostatically attracted by the phosphate groups. This interaction develops in two phases: (1) a co-operative mechanism by which the cysteamine/DNA ratio continuously increases and (2) a saturation effect when this molar ratio reaches the value of 0.5, i.e. when the cysteamine binds to two adjacent phosphate sites [38,39]. We can assume that the binding of the aminothiol to the DNA phosphate groups could prevent secondary double-strand breakdown involved in radiation damage.

Several authors have indicated that peroxidations produced in biological membranes could be revealed by an increase in the fluidity and permeability of the membrane structure [40–42] though some authors do not agree with such a conclusion [43]. The perturbations in enzymatic functions observed after irradiation can be relevant to this increased fluidity of the matrix phospholipids [44], but also and more precisely of the phospholipids surrounding the enzymatic proteins. A similar mechanism has been described in the interaction of local anesthetics with biological membranes [45]. We can imagine that this fluidity could be prevented by the electrostatic binding induced by cysteamine among phospholipid head groups, as described above. The strengthening of the biological membrane would also prevent or delay the burst of lysosomes and the following release of catalytic enzymes secondarily responsible for the cellular death.

In a previous work [7] we had compared the radio-protective activity, after oral administration, of free cysteamine and entrapped cysteamine in egg-yolk lecithine liposomes. Although a protective effect was afforded by entrapped cysteamine (DRF = 1.45), a cysteamine + empty liposomes control test displayed a slight but actual protection (DRF = 1.1). Since cysteamine is known to be inactive when orally administered, on account of its catabolism in the digestive tract, we were led to suggest a direct interaction of the cysteamine on the bilayer polar interface, in this way protecting the unstable SH group. Even if liposomes are not, as they are [46], directly absorbed in the digestive tract, cysteamine may remain trapped in lecithin micelles or sheltered in smaller-sized structures during absorption.

In conclusion cysteamine would appear to be an extremely versatile agent, able to affect beneficially many of the aspects of radiation damage and repair, but most of its cellular effects have not yet come to light. More elaborate investigations into the interaction between cysteamine and biological membranes are necessary to answer the many problems of radiobiology.

Acknowledgements—The authors express their gratitude to Professor M. Ptak and Dr. A. Sanson for helpful and valuable comments. This work was supported by the Direction des Recherches et Etudes Techniques.

REFERENCES

1. W. O. Foye, *Int. J. Sulfur Chem.* **8**, 161 (1973).
2. D. W. Bakkun, in *Progress in Biochemistry and Pharmacology*, Vol. 1, p. 406. Karger, New York (1965).
3. G. G. Jayson, T. C. Owen and A. C. Wilbraham, *J. chem. Soc.* **3**, 944 (1969).
4. L. Novak, *Bull. Acad. R. Belg. U. Sci.* **52**, 633 (1966).
5. D. Vasilescu and M. A. Rix-Montel, *Physiol. Chem. Phys.* **12**, 51 (1980).
6. H. Krank, M. A. Rix-Montel and D. Vasilescu, *Physiol. Chem. Phys.* **13**, 429 (1981).
7. V. Roman, F. Bocquier, F. Leterrier and M. Fatome, *C.R. hebd. Séanc. Acad. Sci., Paris* **295**, 191 (1982).
8. J. Frenzel, K. Arnold and P. Nuhn, *Biochim. biophys. Acta* **507**, 185 (1978).
9. M. Ahmed, J. Hadgraft, J. S. Burton and I. W. Kellaway, *Chem. Phys. Lipids* **27**, 251 (1980).
10. U. Seydel, K. Brandenburg, B. Lindner and H. Moll, *Thermochim. Acta* **49**, 35 (1981).
11. F. Berleur, V. Roman, D. Jaskierowicz, F. Leterrier, A. Esanu, P. Braquet, L. Terminassian-Saraga and G. Madelmont, *Biochem. Pharmac.* **33**, 2407 (1984).
12. A. G. Lee, *Biochim. biophys. Acta* **472**, 237 (1977).
13. A. G. Lee, *Biochim. biophys. Acta* **472**, 285 (1977).
14. W. K. Surewicz and W. Leyko, *Biochim. biophys. Acta* **643**, 387 (1981).
15. B. Kursh, H. Lullmann and K. Mohr, *Biochem. Pharmac.* **32**, 2589 (1983).
16. L. Ter-Minassian-Saraga and G. Madelmont, *FEBS Lett.* **137**, 137 (1982).
17. B. Labbroke and D. Chapman, *Chem. Phys. Lipids*, **3**, 304 (1969).
18. P. D. Garn, in *Thermoanalytic Methods of Investigations*. Academic Press, New York (1965).
19. L. J. Berliner, in *Spin Labeling, Theory and Application*. Academic Press, New York (1976).
20. J. Seelig, *J. Am. chem. Soc.* **92**, 3881 (1970).
21. A. D. Bangham, M. M. Standish and J. C. Watkins, *J. molec. Biol.* **13**, 238 (1965).
22. M. Kerker, in *Scattering of Light and Other Electro-magnetic Radiation*. Academic Press, London (1969).
23. F. Leterrier, F. Berleur, J. Viret and D. Daveloose, *Biorheology Suppl.* **1**, 309 (1984).
24. F. Leterrier and F. Berleur, *Techniques Avancées en Hémo-rhéologie* (Ed. DPIC-INPL), pp. 636–674. Nancy, France (1983).
25. A. D. Keith, G. Bulfield and W. Snipes, *Biophys. J.* **10**, 618 (1970).
26. D. Marsh, in *Spin Labels in Membranes Spectroscopy* (Ed. E. Grell). Springer, Berlin (1981).
27. J. C. Hyde and L. A. Dalton, in *Spin Labeling Theory and Application*, Vol. II (Ed. L. J. Berliner). Academic Press, New York (1979).
28. S. Marbrey and J. M. Sturtevant, *Meth. Membr. Biol.* **9**, 237 (1976).
29. P. N. Yi and R. C. MacDonald, *Chem. Phys. Lipids* **11**, 114 (1973).
30. N. O. Petersen and S. I. Chan, *Biochim. biophys. Acta* **509**, 111 (1978).
31. N. O. Petersen and S. I. Chan, *Biochemistry* **16**, 2651 (1977).
32. W. L. Bergmann, V. Dressler, C. W. M. Haest and B. Deuticke, *Biochim. biophys. Acta* **769**, 390 (1984).
33. A. Sanson, M. Ptak, J. L. Rigaud and C. M. Gary-Bobo, *Chem. Phys. Lipids* **17**, 435 (1976).

34. M. Ptak, M. Egret-Charier, A. Sanson and A. Bouloussa, *Biochim. biophys. Acta* **600**, 387 (1980).
35. H. Broch, D. Cabrol and D. Vasilescu, *Int. J. Quantum Chim.* **7**, 283 (1980).
36. J. Seelig and A. Seelig, *Quat. Rev. Biophys.* **13**, 19 (1981).
37. G. Cohen, R. E. Heikkila, B. Allis, F. Cabbat, D. Dembiec, D. MacNamee, C. Mytilineou and B. Winston, *J. Pharmacol. Exp. Ther.* **199**, 336 (1976).
38. H. Broch, D. Cabrol and D. Vasilescu, *Int. J. Quant. Chem.* **9**, 111 (1982).
39. M. A. Rix-Montel, D. Vasilescu and H. Sentenac, *Studia Biophys.* **69**, 209 (1978).
40. T. Nakazawa, S. Nagatsuka and T. Sakurai, *Int. J. Radiat. Biol.* **40**, 365 (1981).
41. E. Grzelinska, G. Bartosz, K. Gwodzinski and W. Leyko, *Int. J. Radiat. Biol.* **36**, 325 (1979).
42. S. Nagatsuka and T. Nakazawa, *Biochim. biophys. Acta* **691**, 171 (1982).
43. R. C. Bruch and W. Thayer, *Biochim. biophys. Acta* **733**, 216 (1983).
44. D. Papahadjopoulos, K. Jacobson, G. Poste and G. Shepherd, *Biochim. biophys. Acta* **394**, 504 (1975).
45. M. Singer, *Biochem. Pharmac.* **26**, 51 (1977).
46. D. S. Deshmukh, W. D. Bear and H. Brockerhoff, *Life Sci.* **28**, 239 (1981).